



Strategies to improve swine manure hydrochar: HCl-assisted hydrothermal carbonization versus hydrochar washing

Ricardo Paul Ipiales^{1,2} · Andres Sarrion¹ · Elena Diaz¹ · Emiliano Diaz-Portuondo² · Angel F. Mohedano¹ · Angeles de la Rubia¹

Received: 3 November 2022 / Revised: 20 February 2023 / Accepted: 2 March 2023 / Published online: 29 March 2023
© The Author(s) 2023

Abstract

The work focuses on the study of hydrochar upgrading from hydrothermal carbonization (HTC) of swine manure by HCl-assisted HTC or washing with HCl or acetone, as a post-treatment to conventional HTC. Conventional HTC of swine manure yields a low-quality hydrochar (C content ~ 38 wt.%, higher heating value (HHV) ~ 15 MJ kg⁻¹, and ash content up to 32 wt.%). HCl-assisted HTC (0.5 M HCl at 230 °C) substantially reduced the ash content up to ~10 wt.% in the hydrochar and increased the C content to 58 wt.%, reaching a HHV of 23 MJ kg⁻¹. However, the N and S contents remained at values similar to those of the swine manure. Washing post-treatment of conventional hydrochars with HCl or acetone significantly improved the C content and the HHV in the range 47–58 wt.% and 19–25 MJ kg⁻¹, respectively, as well as the ash removal with values 7–11 wt.%. Washing the hydrochar with acetone significantly reduced the N and S contents, obtaining a carbonaceous material with properties suitable for solid biofuel according to ISO/TS 17225–8, (N < 3 wt.%; S < 0.15 wt.%; HHV > 17 MJ kg⁻¹; and ash < 10 wt.%). Hydrochars obtained by HCl-assisted HTC and HCl/acetone washing post-treatment yielded higher thermal stability, as well as better reactivity and low ash agglomeration indexes than compared to conventional hydrochars. Washing post-treatment with acetone proved to be the best strategy to obtain improved hydrochars from swine manure for industrial use as a solid biofuel.

Keywords Acid-assisted hydrothermal carbonization · Energy recovery · Hydrochar quality · Oxidation profiles · Swine manure

1 Introduction

The growing development of the livestock sector, especially the swine sector, has increased the generation of animal manure. Swine manure (SM) is a heterogeneous, dark-colored material composed mainly of fecal matter, urine, feed residues, detergent, bleach, and insecticides, among others. The swine livestock population in European Union (EU; $\approx 142 \times 10^6$ heads) generates $\approx 18 \times 10^6$ t SM per year [1] and released close to 25×10^6 t CO_{2equiv} greenhouse gas (GHG) emissions in 2018 [2]. Swine manure is characterized by a total solid (TS) content 5–10 wt.%, total phosphorus

(P₂O₅) 1–3 kg m⁻³, and total nitrogen 3–8 kg m⁻³ [3, 4]. In addition, SM is a potential energy source due to its high organic matter content, as well as a valuable source of nitrogen and phosphorus. Aerobic composting and anaerobic digestion are two extended procedures for SM management. In EU, 90% of the total animal manure generated is re-applied back to soils as organic fertilizer, although only 30% is properly composted previously [5]. The remaining is directly used without any pretreatment causing several environmental impacts such as runoff, leaching, or eutrophication on aquatic ecosystems such as rivers, groundwater, or ponds [6]. Anaerobic digestion is a suitable approach to valorize animal manure and produce methane-rich biogas. However, the low biodegradability of SM, the presence of inhibitory compounds, the higher ammonia content, the process instability, and the high initial investment make this process inefficient and only valid for intensive farms [7, 8]. In addition, the new environmental policies adopted for the EU limit the use of digestate on agricultural soils [9].

✉ Ricardo Paul Ipiales
ricardo.ipiales@estudiante.uam.es

¹ Chemical Engineering Department, Universidad Autónoma de Madrid, 28049 Madrid, Spain

² Arquimea Agrotech, 28400 Collado Villalba, Madrid, Spain

Hydrothermal carbonization (HTC) is presented as a low-cost alternative for converting biomass with high moisture content into a solid biofuel [10]. HTC has attracted increasing attention due to the inherent merit of direct treatment of wet biomass waste such as animal manure [11, 12], sewage sludge [13, 14], or food waste [15, 16] avoiding the huge amounts of energy required during pre-drying process before pyrolysis or gasification, only suitable when the moisture content does not exceed 5 wt.% [17]. HTC operates at relative low temperature (180–250 °C), residence time (5–240 min), and autogenous pressure generating as mainly product a carbon-rich solid called hydrochar, a liquid by-product with high content of soluble organic compounds, minerals, and nutrients called process water, and a minimal fraction of non-condensable gases mainly consisting of CO₂ and H₂O [18]. HTC contributes to improve the properties of the raw biomass, although in some cases the hydrochar obtained does not reach characteristics suitable for use as a solid biofuel (low HHV and high ash, N, and S contents). HTC decreases the Na and K contents in the resulting hydrochar, which could reduce ash agglomeration and fouling risk [19]. In the case of biomass rich in N-NH₃, alkali metals (Ca, Mg, and P), and hydrolyzable compounds (carbohydrates, proteins and fat) such as sewage sludge, animal manure, or microalgae, HTC generates alkaline process water, which increases the formation of insoluble metal complexes that are retained in the hydrochar [13, 20–22].

Acid-assisted HTC (HTC-A) is an effective alternative to conventional HTC, to improve the physicochemical properties of the hydrochar by extending charring, ash elution, deamination, and desulfurization of the raw biomass [12, 23, 24]. Some authors highlighted the leaching of N and P to the liquid fraction in HTC-A, which facilitates the recovery of nutrients from the process water as phosphate salts after neutralization [23–25]. Another pathway to improve the hydrochar properties as well as ash, N, and S removal is the hydrochar washing [26, 27].

In the present study, two strategies are studied to improve the properties of swine manure hydrochar: (i) a washing post-treatment of hydrochar, with HCl or acetone, from conventional HTC hydrochar at different carbonization temperatures, and (ii) HCl-assisted HTC at different concentrations and temperatures. In each case, the characteristics of the hydrochar obtained are analyzed by proximate and ultimate analysis, and inductively coupled plasma atomic emission spectroscopy to elucidate the effects of temperature, acid concentration, and solvent type. Ash agglomeration indexes and hydrochar

combustion characteristics are also evaluated to obtain a solid biofuel for industrial use.

2 Materials and methods

2.1 Feedstock origin

The SM was collected from an intensive swine farm (Avila, Spain) and stored at –20 °C without any pretreatment. The main characteristics of the raw material are shown in Table 1.

2.2 Hydrothermal carbonization experiments

Hydrothermal experiments were carried out in a 4-L ZipperClave® pressure vessel, electrically heated at a heating rate of 3 °C min⁻¹, at three temperatures (180, 210, and 230 °C). Once the reaction temperature had been reached, the residence time for all the tests was 1 h. The time to reach the reaction temperature depended on the target temperature of the test. After the reaction, the reactor was cooled by an internal coil using tap water with a cooling rate of 10 °C min⁻¹. Conventional HTC tests were performed by duplicate. The slurry (hydrochar + process water) was separated by centrifugation (Orto Alresa; Madrid, Spain) at 8000 rpm for 10 min and filtration (0.45 µm). The wet hydrochar was dried at 105 °C, ground, and sieved (<250 µm). The hydrochar resulting from conventional HTC were labeled as HC followed by the reaction temperature (i.e., HC180, HC210, and HC230). These hydrochars were washed with HCl (Wa) or acetone (Wb) according to the following procedure: (i) 2 g of HC180, HC210, and HC230 was stirred at 25 °C for 2 h with 20 mL of 5-M HCl; and (ii) 2 g of HC180 was stirred at 25 °C for 2 h with 20 mL of a 20%, 50%, or 75% (v:v) solution of acetone. The suspension was filtered (0.45 µm) and each hydrochar was rinsed with deionized water to neutral pH and dried at 105 °C. The HCl-washed hydrochars (HC-Wa)

Table 1 Main characteristics of swine manure¹

		Mineral metals (g kg ⁻¹)		Heavy metals (mg kg ⁻¹)	
FC (%)	15.7 (0.1)	Al	1.4 (0.0)	Cd	1.8 (0.0)
VM (%)	60.0 (0.1)	Ca	31.2 (0.1)	Cr	9.8 (0.1)
Ash (%)	24.3 (0.3)	Fe	1.6 (0.0)	Cu	137.0 (5.0)
C (%)	35.6 (0.4)	K	35.4 (0.0)	Ni	4.1 (0.6)
N (%)	2.4 (0.1)	Mg	13.1 (0.2)	Pb	3.2 (0.0)
S (%)	0.7 (0.1)	Na	10.2 (0.0)	Zn	111.2 (2.1)
HHV (MJ kg ⁻¹)	14.5 (0.3)	P	30.7 (0.2)		

¹Average values of 3 determinations with standard deviations in brackets

were labeled as HC180-Wa, HC210-Wa, and HC230-Wa, respectively, while the acetone-washed hydrochars (HC-Wb) were labeled as HC180-Wb-20, HC180-Wb-50, and HC180-Wb-75, respectively, according to the concentration of acetone in the washing solution. Hydrochar washing assays, with HCl or acetone, were performed in duplicate.

A second series of experiments were performed by acid-assisted HTC at 180 °C for 1 h using 0.1-, 0.25-, 0.5-, and 1.0-M HCl and also at 210 and 230 °C for 1 h with 0.5-M HCl. The hydrochars obtained were labeled according to HTC temperature and acid concentration (i.e., HC-A-180–0.1, HC-A-180–0.25, HC-A-180–0.5, HC-A-180–1.0, HC-A-210–0.5, and HC-A-230–0.5).

2.3 Feedstock and hydrochar characterization

Swine manure and hydrochar were characterized by elemental composition (C, H, N, and S) using a CHNS analyzer (LECO CHNS-932; Geleen, The Netherlands). Proximal analysis (moisture, ash, volatile matter (VM), and fixed carbon (FC)) was performed using a Discovery SDT thermogravimetric analyzer (TG 209, F3, Netzsch; Selb, Germany) according to ASTM-D7582 [28]. Oxygen (O) in the elemental analysis was calculated by difference ($100 - C - H - N - S - \text{ash}$ (wt.%)). Finally, metal (mineral and heavy) composition was determined by inductively coupled plasma atomic emission spectroscopy (ICP-OES) on an Elan 6000 Sciex instrument (Perkin Elmer; Santa Clara, USA). The determination of the main characteristics of feedstock and hydrochars was performed in triplicate. Hydrochar mass yield (Y_{HC}) was calculated as the ratio of weight of hydrochar recovered (W_{HC}) to the weight of feedstock (W_{SM}), both on a dry basis (Eq. 1).

$$Y_{\text{HC}}(\%) = \frac{W_{\text{HC}}}{W_{\text{SM}}} \cdot 100 \quad (1)$$

The HHV of the dry solid samples was determined using the Eq. 2 [19], where the concentration of C, H, S, N, O, and ash is expressed as wt.% on a dry basis:

$$\text{HHV} (MJ \text{ kg}^{-1}) = 0.3491 \cdot C + 1.033 \cdot H + 0.1005 \cdot S - 0.0151 \cdot N - 0.103 \cdot O - 0.0211 \cdot \text{Ash} \quad (2)$$

The energy yield (E_{yield}) of hydrochar was calculated using Eq. 3:

$$E_{\text{yield}}(\%) = Y_{\text{HC}}(\%) \cdot \frac{\text{HHV}_{\text{HC}}}{\text{HHV}_{\text{SM}}} \quad (3)$$

2.4 Oxidation and thermal reactivity profiles of hydrochars

The thermogravimetric analysis (TG) and derivative thermogravimetric (DTG) were carried out in a thermogravimetric analyzer (Discovery SDT 650). The samples were heated from 25 to 900 °C with an air flow rate of 100 mL min⁻¹ and a heating rate of 10 °C min⁻¹. Ignition temperature (T_i), burnout temperature (T_b), and peak temperature of the maximum loss weight (T_m) are characteristic parameters of combustion and reflect the thermal behavior of fuels during the combustion process. The comprehensive combustibility index (CCI; Eq. 4), and fuel ratio (FR; Eq. 5) describes the intensity and stability during the oxidation, respectively [29].

$$\text{CCI} (\text{min}^{-2} \cdot ^\circ\text{C}^{-3}) = \frac{(\text{dw}/\text{dt})_{\text{max}} - (\text{dw}/\text{dt})_{\text{mean}}}{T_i^2 \cdot T_b} \quad (4)$$

where $(\text{dw}/\text{dt})_{\text{max}}$ indicates maximum weight loss rate and $(\text{dw}/\text{dt})_{\text{mean}}$ the average weight loss rate (wt.% min⁻¹) and T_i and T_b correspond to ignition temperature and burn out temperature (°C), respectively.

$$\text{FR} = \frac{\text{FC} (\%)}{\text{VM} (\%)} \quad (5)$$

2.5 Ash fouling and slagging prediction

Slagging and fouling indexes (Table 2) were calculated based on the ash composition according to the equations described by Cao et al. [30].

2.6 Mass balance and element distribution

The distribution of elements in the hydrochar and process water was determined by mass balance, following Eqs. 10 and 11:

$$X_{\text{HC}}(\%) = \frac{X_{i\text{HC}} \cdot W_{\text{HC}}}{X_{i\text{SM}} \cdot W_{\text{SM}}} \cdot 100 \quad (10)$$

$$X_{\text{pw}}(\%) = \frac{X_{i\text{PW}} \cdot W_{\text{PW}}}{X_{i\text{SM}} \cdot W_{\text{SM}}} \cdot 100 \quad (11)$$

where X_i is the mass fraction of elements in the hydrochar, process water, or swine manure and W_{HC} , W_{PW} , and W_{SM} are the mass of hydrochar, process water recovered after filtration, and swine manure, respectively. The C content in the gas phase was calculated by mass balance.

The data obtained were assessed by analysis of variance (ANOVA) using Origin software (version 9.1). Fisher's

Table 2 Slagging and fouling equations

Slagging and Fouling Index	Equation	Limits	Eq.
Acid Base Ratio ($R_{b/a}$)	$R_{b/a} = \frac{Fe_2O_3 + CaO + MgO + P_2O_5 + K_2O + Na_2O}{SiO_2 + Al_2O_3 + TiO_2}$	$R_{b/a} < 0.5$, low slagging risk $0.5 < R_{b/a} < 1$ medium slagging risk $1 < R_{b/a} < 1.75$ high slagging risk $R_{b/a} > 1.75$ severe slagging risk	(6)
Slagging index (SI)	$SI = R_{b/a} \cdot S_d$	$SI < 0.6$ low slagging inclination $0.6 < SI < 2.0$ medium $2.0 < SI < 2.6$ high $SI > 2.6$ extremely high	(7)
Fouling index (FI)	$FI = R_{b/a} \cdot (K_2O + Na_2O)$	$FI < 0.6$ low fouling inclination $0.6 < FI < 40.0$ medium $FI > 40.0$ high propensity	(8)
Alkali Index (AI)	$AI \text{ (kg GJ}^{-1}\text{)} = \frac{(K_2O + Na_2O) \cdot Ahs}{HHV \text{ (GJ kg}^{-1}\text{)}}$	$AI < 0.17$ safe combustion $0.17 < AI < 0.34$ possible slagging and fouling $AI > 0.34$ virtually certain slagging and fouling	(9)

S_d is the sulfur content (wt.%) on a dry basis

least significant difference (Fisher's LSD) was calculated at a confidence level of 0.05.

3 Results and discussion

Figure 1 shows the fate of C, N, and S in HTC products, expressed on percentage. Increasing reaction severity (temperature and acid concentration) increased the C content in the gas phase, probably due to decarboxylation reactions [31]. C release into the gas phase was around 6–8%. The temperature increase hardly varied the C retained in hydrochar from 60 to 56%, while the addition of acid at the lowest concentration (0.1 M HCl) and temperature (180 °C) reached the lowest C content in hydrochar ~46% (Fig. 1a). The increase in acid concentration and reaction temperature improved the C sequestration in the hydrochar which remained in the range of 48–59 wt.%. The acid presence and rise temperature could have increased the hydrolysis reactions of the SM [3, 13]; thus, more C is released into the liquid fraction, however as well favored the recondensation and polymerization of the soluble organic compounds in the process water which results in the formation of secondary hydrochar [3, 20, 32–34], increasing the C in the hydrochar. The presence of HCl in the HTC reactions changes the zeta potential, which is a key indicator of the stability of colloidal dispersions that measures the degree of particle repulsion [34]. Baccile et al. [35] determined the zeta potential in swine manure HTC at different pH and evidenced that low pH results in a negative zeta potential; thus, particles and compounds in suspension tended to agglomerate, leading to secondary hydrochar. Hence, the addition of HCl appears to have a catalytic effect on HTC reactions both promoting the hydrolysis of the organic compounds of

the feedstock and the recondensation and polymerization of soluble compounds. The N content of hydrochar increased from 44 to 62 wt.% in HTC180 and HTC-A-210–0.5, respectively, while the organic N content (Org-N) decreased to disappear with increasing acid concentration and temperature. Org-N (proteins and amino acids) was mainly converted into N-NH₃, which increased slightly by temperature ~4 percentage points (p.p.), while by acid action, increases of up to 12 p.p. were observed. The N-NO₂ and N-NO₃ accounted for less than 0.1% of the total nitrogen in the process water. The increase in N retained in hydrochar may be due to the adsorption of nitrogenous compounds from the process water onto the hydrochar [9, 36, 37] or to the formation of secondary hydrochar, where nitrogenous compounds (aromatics and heterocycles) play an important role [20, 38]. The S shows a high migration rate > 50 wt.% into the process water as SO₄²⁻ by desulfurization reactions [39].

Table 3 shows the elemental and proximal analysis of hydrochars. The Y_{HC} decreased significantly with increasing temperature, varying from 55.5 wt.% HC180 to 50.7% HC230, while 32% of the hydrochar mass corresponded to ash. Hydrochar washing caused a mass loss of 20–35 wt.% mainly attributed to ash removal, diminishing the Y_{HC} to 36.2–38.0 wt.% and 42.1–44.2 wt.%, for acid and acetone, respectively. Acetone washing appears to have the same effect on ash removal, regardless of the solution concentration. In the acid-assisted HTC, the increase in acid concentration reduced drastically the Y_{HC} from 41.5 (HC-A-180–0.1) to 26.4 wt.% (HC-A-180–1.0), while the increment in the temperature showed a minimal effect on Y_{HC} from 39.7 (HC-A-180–0.5) to 38.1 wt.% (HC-A-230–0.5). The hydrochar mass loss was attributed to the action of HCl as catalyst on hydrolysis reactions [24, 30], increasing the mass loss rate and the transfer of molecular compounds into the liquid

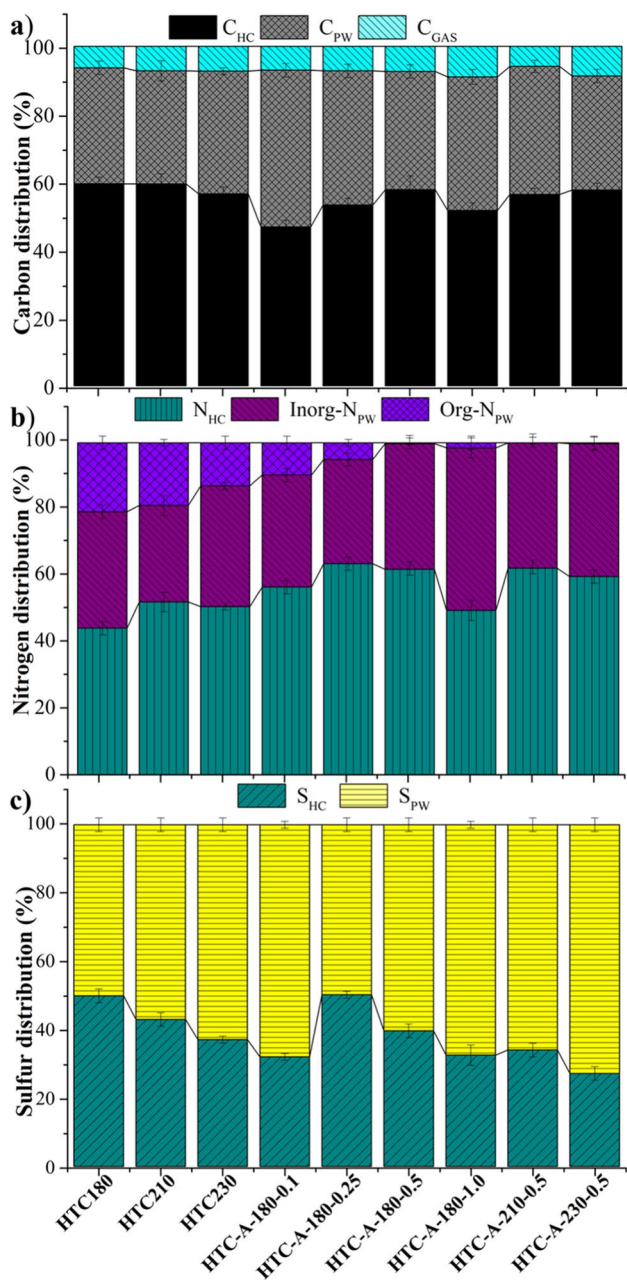


Fig. 1 Fate of carbon (a), nitrogen (b), and sulfur (c) in hydrochar, process water, and gas phase from conventional and acid-assisted HTC

fraction in the case of HTC-A and solubilization of metals into the process water in the case of HTC-A and hydrochar washing (see Figs. 2 and 3).

In addition to the hydrolysis reactions, decarboxylation and dehydration reactions took place along the HTC of SM, leading to a loss of H and O in the form of CO₂ and H₂O, respectively. The C content increased slightly by HTC temperature from 35.6 (SM) to 39.0 wt.% (HC230), while the highest C content (~58 wt.%) was obtained

Table 3 Main characteristics of hydrochars from conventional HTC, washing post-treatment, and HCl-assisted HTC in dry basis (wt.%)

		Y _{HC} (%)	FC (%)	VM (%)	Ash (%)	C (%)	N (%)	S (%)	HHV (MJ kg ⁻¹)	E _{yield} (%)
Conventional HTC	HC180	55.2 ^g (1.2)	14.4 ^{cd} (0.1)	53.9 ^a (0.1)	31.6 ^g (0.2)	37.6 ^a (0.1)	1.9 ^{ab} (0.0)	0.6 ^b (0.0)	15.5 (0.2)	60.6 (0.2)
	HC210	54.1 ^g (1.1)	15.3 ^{cd} (0.1)	52.1 ^a (0.1)	32.4 ^g (0.2)	38.3 ^a (0.2)	2.3 ^c (0.1)	0.5 ^b (0.0)	15.7 (0.1)	60.3 (0.5)
	HC230	50.7 ^g (1.0)	15.8 ^d (0.3)	51.5 ^a (0.1)	32.6 ^g (0.1)	39.0 ^b (0.2)	2.3 ^c (0.1)	0.5 ^b (0.0)	15.8 (0.2)	56.6 (0.3)
HCl washing	HC180-Wa	38.5 ^{de} (0.5)	19.2 ^e (0.1)	73.4 ^{cd} (0.1)	7.3 ^a (0.1)	52.7 ^{cd} (0.1)	2.3 ^c (0.1)	0.7 ^b (0.0)	22.6 (0.3)	61.6 (0.3)
	HC210-Wa	36.2 ^d (1.2)	21.9 ^f (0.1)	70.3 ^{bc} (0.1)	7.7 ^a (0.1)	55.2 ^d (0.2)	2.8 ^d (0.1)	0.8 ^{bc} (0.0)	23.7 (0.1)	62.1 (0.2)
	HC230-Wa	38.0 ^{cd} (0.6)	25.2 ^f (0.1)	63.9 ^{bc} (0.1)	10.8 ^{cd} (0.1)	57.8 ^d (0.3)	3.1 ^d (0.1)	0.9 ^c (0.0)	25.1 (0.1)	49.8 (0.3)
Acetone washing	HC180-Wb-20	44.2 ^f (1.5)	19.6 ^{ef} (0.2)	71.5 ^{cd} (0.1)	8.7 ^b (0.1)	47.5 ^{bc} (0.1)	1.8 ^{ab} (0.1)	0.1 ^a (0.0)	18.8 (0.1)	59.8 (0.3)
	HC180-Wb-50	43.4 ^{ef} (2.5)	19.5 ^{ef} (0.1)	69.1 ^{bc} (0.1)	11.3 ^d (0.1)	47.1 ^{bc} (0.1)	1.7 ^b (0.1)	0.1 ^a (0.0)	18.7 (0.1)	60.6 (0.1)
	HC180-Wb-75	42.1 ^{def} (1.1)	21.9 ^f (0.1)	69.1 ^{bc} (0.1)	8.8 ^b (0.1)	47.2 ^{bc} (0.1)	1.9 ^{a,b} (0.1)	0.1 ^a (0.0)	18.5 (0.2)	56.0 (0.2)
HCl-assisted HTC	HC-A-180-0.1	41.5 ^{def} (1.1)	12.4 ^b (0.1)	70.8 ^{cd} (0.2)	16.7 ^f (0.1)	39.1 ^a (0.1)	3.24 ^e (0.1)	0.5 ^b (0.0)	14.8 (0.2)	43.6 (0.3)
	HC-A-180-0.25	43.1 ^{ef} (1.2)	14.2 ^c (0.1)	69.7 ^b (0.2)	16.0 ^f (0.1)	42.4 ^b (0.2)	3.5 ^c (0.1)	0.8 ^{bc} (0.0)	17.0 (0.1)	52.0 (0.3)
	HC-A-180-0.5	39.7 ^{de} (1.0)	15.3 ^{cd} (0.1)	70.6 ^b (0.1)	14.0 ^e (0.1)	49.5 ^b (0.2)	3.7 ^{cf} (0.2)	0.7 ^b (0.0)	21.2 (0.1)	63.8 (0.5)
	HC-A-180-1.0	26.4 ^h (0.5)	9.5 ^a (0.1)	73.6 ^{cd} (0.1)	15.7 ^f (0.1)	50.3 ^b (0.3)	3.6 ^{cf} (0.2)	0.7 ^b (0.0)	23.6 (0.1)	38.6 (0.2)
	HC-A-210-0.5	32.8 ^h (0.6)	11.8 ^b (0.1)	72.4 ^{cd} (0.1)	15.6 ^{ef} (0.1)	55.1 ^d (0.2)	3.9 ^{ef} (0.0)	0.6 ^b (0.0)	20.8 (0.1)	53.1 (0.3)
	HC-A-230-0.5	38.1 ^{cd} (0.5)	12.8 ^b (0.1)	77.2 ^d (0.1)	9.9 ^e (0.1)	57.7 ^d (0.1)	4.0 ^f (0.1)	0.7 ^b (0.0)	22.8 (0.1)	65.6 (0.3)

^{a,b,c,d,e,f,g} Average values of three determinations with standard deviations. Means with different superscript significant differ (*p* < 0.05)

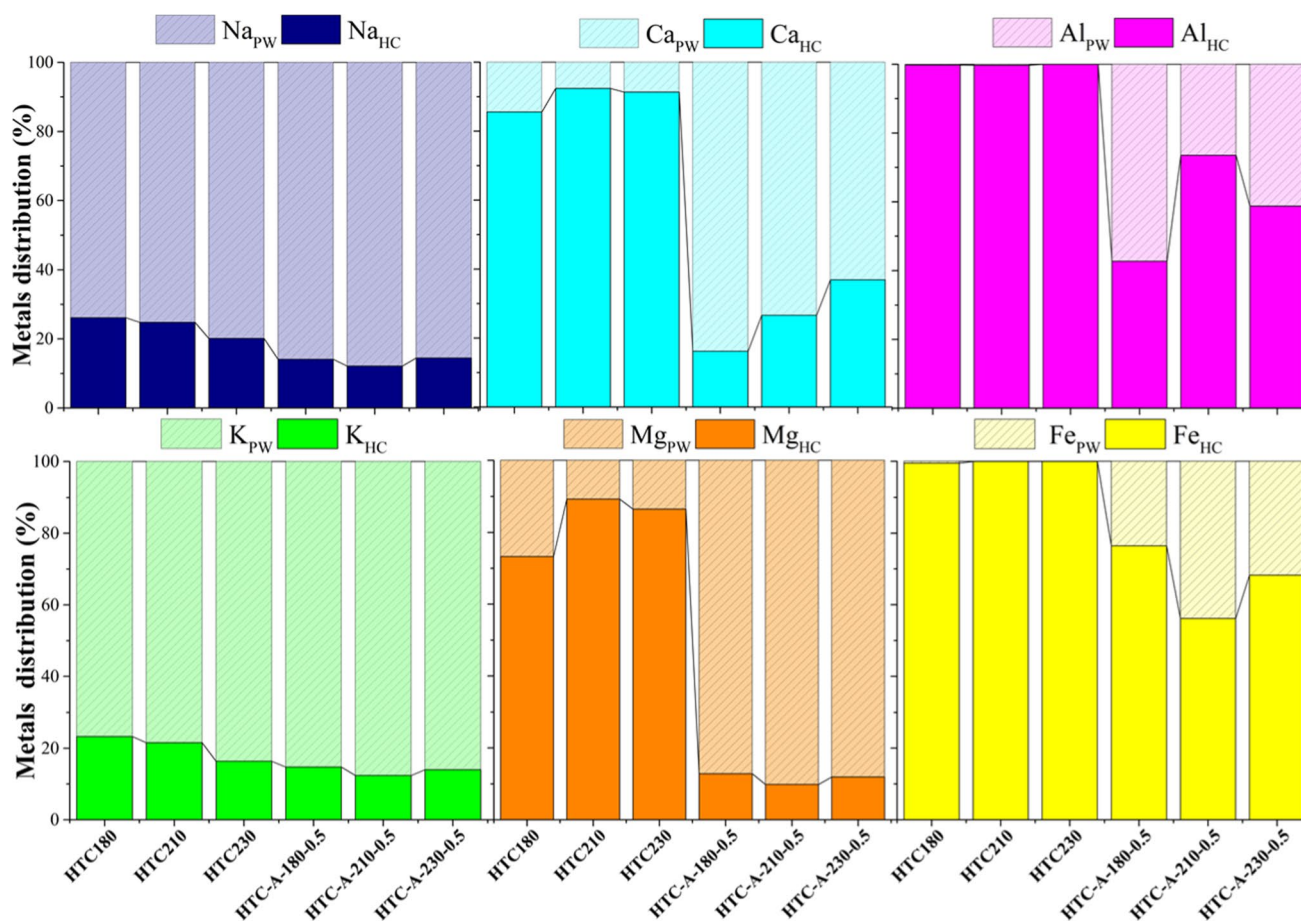


Fig. 2 Fate of metals in hydrochars and process waters from conventional and acid-assisted HTC

in HC230-Wa and HC-A-230–0.5, due to ash removal by hydrochar washing, or ash elution from SM in acid-assisted HTC. Acetone concentration used in the hydrochar washing showed no effect on C content (~ 47 wt.%); however, acid concentration and temperature in HTC-A showed a strong effect on C content increasing from 39.1 (HC-A-180–0.1) to 50.3 wt.% (HC-A-180–1.0) and from 49.5 (HC-A-180–0.5) to 57.7 wt.% (HC-A-230–0.5), respectively. A slight reduction of N from 2.4 (SM) to 1.9–2.3 wt.% and S from 0.7 (SM) to 0.5–0.6 wt.% content was observed in hydrochar from conventional HTC by deamination and desulfurization reactions. Hydrochar washing showed a different effect in the N and S contents. Washing post-treatment of hydrochar with HCl did not modify and even increased the N (2.3–3.1 wt.%) and S (0.7–0.9 wt.%) contents, while acetone washing decreased the content of both elements below 2 wt.% and 0.15 wt.%, respectively, due to the high solubility of organic compounds in organic solvents (Table 3). The hydrochar structure usually consists of a wide diversity of N-bearing (pyridine and imidazole) or S-bearing (thiols, thioethers, and thioacetals) species [40, 41], which are soluble in polar

solvents such as acetone. Polar solvents such as N-dimethylformamide (DMF), ethylene glycol, and dichloromethane (DCM), among others, are commonly used to remove N- and S-containing organic compounds from fuels such as kerosene, gasoline, or diesel [42, 43]. Finally, acid-assisted HTC significantly increased the N (3–4 wt.%) and moderately the S (0.5–0.8 wt.%) contents.

The increase in the C content improved HHV from 14.5 in SM to 25.1 MJ kg⁻¹ in HC230-Wa and 23.6 MJ kg⁻¹ in HC-A-180–1.0. Since the increase in HHV implies a decrease in Y_{HC} , the E_{yield} is a better reference of potential energy recovery from hydrochar. The highest E_{yield} was obtained in HC-A-230-0.5 (65.6%), followed by HC-A-180-0.5 (63.8%) and HC180-Wa and HC210-Wa (~ 62%). The lowest E_{yield} was obtained in HC-A-180-0.1 (43.6%) followed by HC-A-180-1 (38.6%); although these hydrochars showed a high HHV, their low Y_{HC} (~ 30 wt.%) caused a considerable energy recovery decrease. Conventional HTC resulted in a slight decrease in VM, from 60 in SM to ~ 51–55 wt.% in hydrochar, and an increase in ash content, from 24 to ~ 32 wt.%, respectively, while the FC was maintained ~ 15 wt.%, regardless of carbonization temperature.

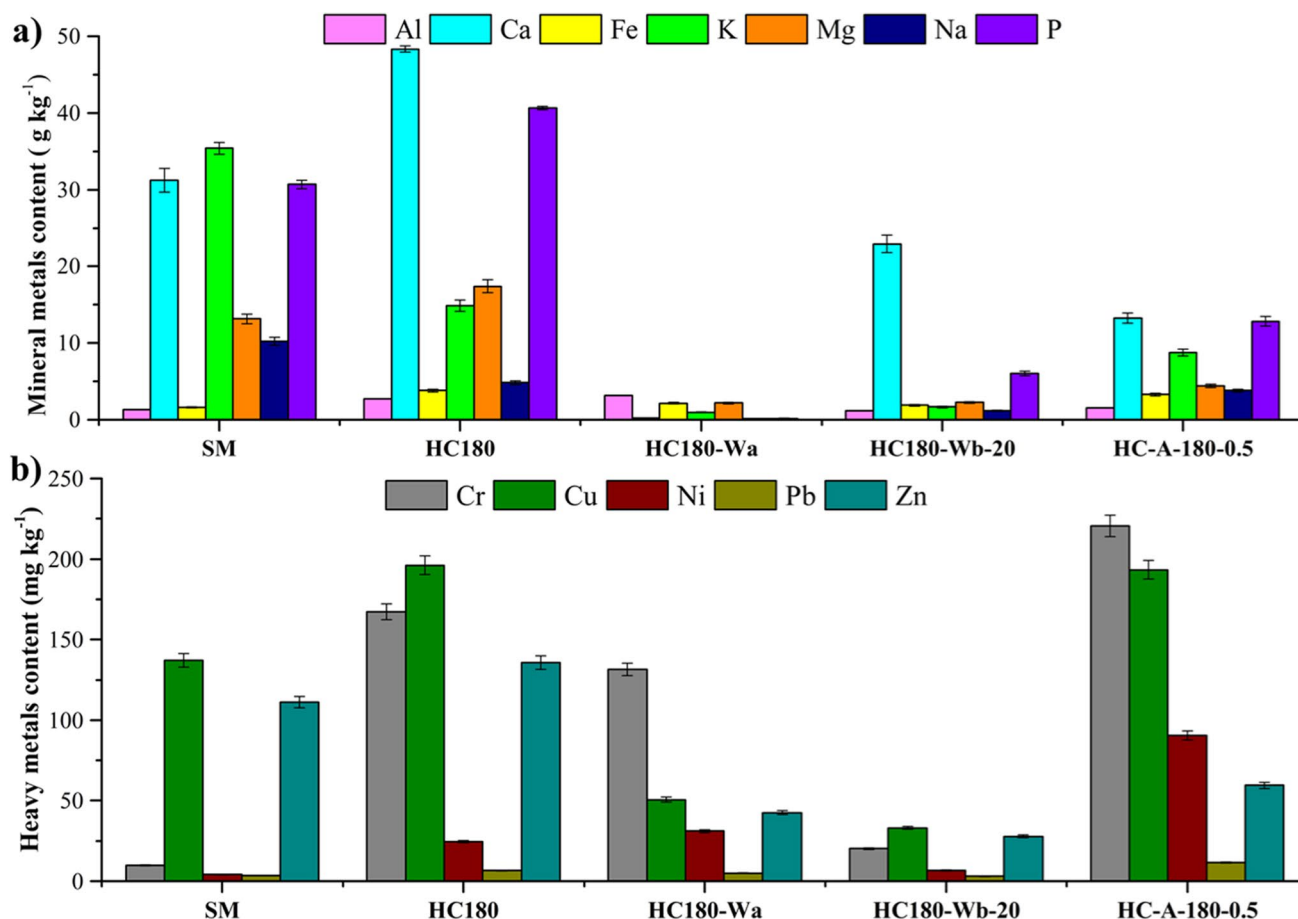


Fig. 3 Mineral (a) and heavy metals (b) in swine manure, HC180, HC180-Wa, HC180-Wb, and HC180-0.5

The increase in ash content in hydrochar from conventional HTC was related to the basic pH of the process water (≈ 9), which decreased metal solubilization (specially polyvalent metals; see Fig. 2) and promote the formation of insoluble salts [25, 44, 45]. Previous studies have shown that high P content from raw feedstock leads insoluble phosphorus salts (Ca-, Mg-, Al-, and Fe-phosphates) which are retained on the hydrochar structure [9, 33]. Phosphorus retained in the hydrochar reached up to 92% (close to 40 g P kg⁻¹ HC) in conventional HTC. On other hand, VM and FC in washed hydrochar and VM in acid-assisted hydrochar increased with decreasing ash content. Hydrochar washing diminished the ash content to values 7.3–11.3 wt.%, considerably lower than those observed for SM (~ 24 wt.%) or hydrochar (~ 32 wt.%). Acid washing proved to be a better option than acetone washing, achieving a 70 wt.% and 60 wt.% ash removal, respectively. Likewise, acid-assisted HTC enhances the leaching of metallic elements during the carbonization process by transferring cations and anions into the process water, increasing the carbon content and HHV of the resulting hydrochar. The solution pH in all process water from HTC-A was < 3 . A pH < 5 implies high

solubility of salts [37], and, therefore, the mass loss after washing with acid was due to migration of dissolved ions to the liquid fraction. The ability of organic solvents such as DMF, DCM, or ethanol to form metal complexes due to the difference in redox potentials between the solvent and the metal ion is well known [26, 46, 47]. Figure 3 shows the ability of acetone to remove high metal content regardless of the concentration used. This effect on ash removal could not be evidenced in acetone-assisted swine manure HTC [34] which could be due to the lower stability of acetone under subcritical conditions, which could degrade or be involved in HTC reactions.

Figure 2 shows the distribution of majority of mineral metals in hydrochar and process water from conventional HTC and acid-assisted HTC at different temperatures. In conventional HTC, monovalent metals were solubilized in the process water (83 wt.% K and 79 wt.% Na), while divalent (Ca and Mg) leached to a lesser extent (~ 20 wt.%), and Al and Fe remained unchanged in the solid fraction. Acid-assisted HTC favored the leachate of less soluble metals to process water (up to 80 wt.% for Ca and 90 wt.% for Mg and close to 60 wt.% for Al and 40 wt.%

for Fe) and enhanced the solubilization of K and Na up to 90 wt.%. In this case, increasing the temperature decreased metal solubilization (~ 25% on average) except for monovalent metals that decreased even with the increment in the temperature. Increased temperature results in higher metal complexation, whereby more ash is retained in the hydrochar structure [15, 48].

Figure 3 shows metal content of SM, HC180, HC180-Wa, HC180-Wb, and HC-A-180-0.5. Hydrochar obtained at the lower HTC temperature was selected to evaluate the metal content in all the cases. Monovalent metals in HC180 showed a moderate reduction (Na ≈ 30 wt.% and K ≈ 60 wt.%) due to their high solubilization (Fig. 2). Polyvalent metals such as Ca, Mg, Al, Fe, and P showed an opposite trend increasing in all cases (~ 40 wt.% in average). Similar trend to polyvalent metals was observed for the heavy metals content. The increase in temperature promoted metal retention in the hydrochar, which resulted in an increase in ash content (Table 3 and Fig. 2). Hydrochar washing leads to different effects in the solubilization of mineral and heavy metals compared to HC180. HCl washing removed almost all mineral metal content (up to 90 wt.% was removed, except Al which remained constant), while acetone washing also removed 80 wt.% mineral metals, except for Ca (55 wt.%).

On the contrary, the heavy metal removal was better with acetone washing (up to 80%), than with HCl washing (~ 50 wt.% in average), as compared with HC180. On other hand, acid-assisted HTC showed a less intense effect on mineral metals remove (up to 70 wt.%) and promoted heavy metal content increase compared to HC180. The increment in the metal content can be explained by the Y_{HC} of acid-assisted hydrochar, showing a severe reduction due to the acid addition, which catalyzed the hydrolysis, decarboxylation, and dehydration reactions in SM-HTC. These reactions caused an increase in the metal concentration compared to those washed with HCl or acetone, due to the loss of carbon from the solid phase into the liquid phase. Hydrochar washing with HCl or acetone only affected the metal content retained in conventional hydrochar, but not the carbon content.

Figure 4 shows the TG and DTG profiles of the feedstock, HC180, HC180-Wa, HC180-Wb, and HC-A-180-0.5, where three different peaks are observed for each hydrochar (except HC-A-180-0.5). The first peak corresponds to moisture loss, from 60 to 150 °C with a weight loss of less than 5 wt.% in all cases. The second peak corresponds to the oxidation of VM, cellulose, and hemicellulose, with different weight loss depending on the hydrochar considered. The feedstock and

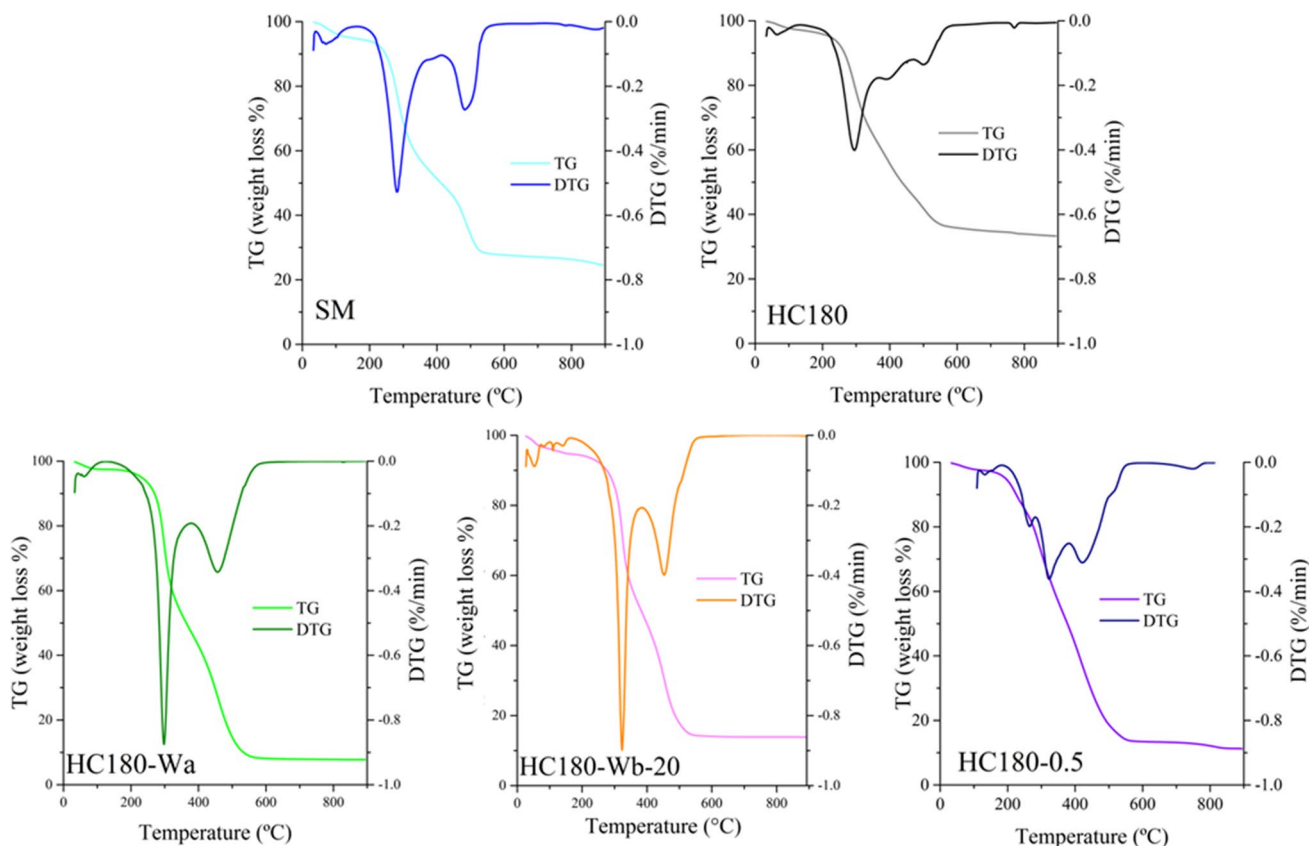


Fig. 4 TG and DTG profiles of swine manure and hydrochars

conventional hydrochars presented a weight loss ~ 35 wt.%, while HC-Wa and HC-Wb presented the highest mass loss (higher than 60 wt.%). The third peak corresponds to the oxidation of long-chain and thermally stable compounds, such as FC and lignin, with a weight loss of up to 20 wt.%. HC180 shows a poorly defined FC peak, probably due to the high ash content of the hydrochar, while in the rest of the hydrochars, due to the low ash content, the FC peak is clearer. Likewise, HC-A-180–0.5 presented an amorphous form with poorly defined but overlapping peaks. The absence of a peak suggests that the cellulose, hemicellulose and VM were partially removed by the HCl during the HTC reactions. One DTG peak suggests slow and partial oxidation, whereas the two-peak progression of the reaction denotes a rapid stage of devolatilization and oxidation of hydrochar [49]. The two-stage oxidation could prevent the formation of NO_x and SO₂ [34], two of the most pollutant GHG. Overall, feedstock and conventional hydrochars presented the lowest weight loss (~ 65 wt.%) due to high ash content, while HC-Wa, HC-Wb, and HC-A reached oxidation values ≈ 90 wt.%, which results in lower ash generation, and would avoid ash agglomeration problems in the combustion chambers.

Table 4 shows oxidation analysis of hydrochar. Conventional hydrochar showed a slight T_i increase (up to 10 °C), compared to SM. Washed hydrochar and acid-assisted hydrochar showed opposite behaviors, while washed hydrochar yielded an increase of T_i (between 7 and 29 °C); the one obtained by acid-assisted HTC showed the lowest values of T_i (up to 40 °C lower) compared to conventional hydrochar. Although the VM content remains in a constant range, the FC content varies according to hydrochar pre- or post-treatment, which is reflected in the FR. The FR increased from 0.26 in SM to 0.40 in HC230-Wa and decreased in acid-assisted hydrochar (<0.20), which shows

that conventional hydrochars and washes hydrochar are thermally more stable, while HC-A are more reactive. The higher reactivity of HC-A was probably due to the presence of secondary hydrochar which usually remains in the external layer of the hydrochar [49, 50]. In the use of hydrochar as an alternative biofuel in blending with coal, it is not enough that hydrochar has a high calorific value but also a similar oxidation behavior to avoid segregation or divergence in the combustion of the two materials. Similar oxidation behaviors would allow to obtain a higher stability and complete oxidation, flame ignition stability, and avoid formation of N and S oxides [20, 49]. The CCI indicated that all types of hydrochar showed better combustion performance compared to SM; therefore, the use of hydrochar in solitary or in blend with coal is a suitable alternative for energy recovery [51].

Conventional hydrochar decreased FI, SI, and AI compared to SM, although not enough to avoid the mentioned problems, specially SI, $R_{b/a}$ and AI (Table 4), being less interesting for combustion. Hydrochar washing reduced all the indexes to medium and low values (AI < 0.2, SI < 2, and FI < 0.6), in the range of the suitable for combustion, while acid-assisted hydrochar presented SI, FI, and AI values in the range of moderate ash agglomeration for combustion, especially by the high S content, which is one of the main causes of agglomeration and corrosion produced by ashes and, consequently, of rapid fouling and ash coating in combustion boilers [52, 53]. The presence of acid in the reaction was favorable ash removal in terms of fouling and slagging, strongly decreasing the ash agglomeration indexes, nevertheless, the inability to remove S of the hydrochar; the indexes were in the range of high medium values. Overall, hydrochar washing appears as an interesting strategy to decrease the slagging and fouling problems followed by HTC-A being

Table 4 Ash agglomeration indexes and combustion characteristics of hydrochars

	T_i (°C)	T_m (°C)	T_b (°C)	FR	CCI·10 ⁷ (min ⁻² °C ⁻³)	$R_{b/a}$	SI	FI	AI (kg GJ ⁻¹)
SM	231 ^b (3)	281 ^a (1)	573 ^a (4)	0.26	9.2	35.8	26.1	9.0	4.3
HC180	241 ^{b,c} (2)	295 ^{a,b} (1)	658 ^b (4)	0.27	6.2	24.3	16.0	2.1	1.8
HC210	241 ^{b,c} (4)	301 ^{a,b} (4)	674 ^b (2)	0.29	5.6	24.5	14.2	1.4	1.5
HC230	236 ^{b,c} (3)	294 ^{a,b} (3)	647 ^b (2)	0.31	5.8	29.5	15.8	1.8	1.2
HC180-Wa	243 ^{b,c} (4)	297 ^{a,b} (4)	715 ^{b,c} (2)	0.26	8.9	1.3	0.9	0.1	0.2
HC210-Wa	247 ^{b,c} (3)	291 ^{a,b} (4)	794 ^c (4)	0.31	6.3	1.7	1.4	0.1	0.2
HC230-Wa	260 ^c (1)	291 ^{a,b} (2)	746 ^c (3)	0.40	7.0	2.0	1.8	0.1	0.2
HC180-Wb-20	268 ^c (4)	323 ^b (2)	553 ^a (4)	0.27	10.6	1.6	0.2	0.2	0.1
HC180-Wb-50	270 ^c (3)	324 ^b (4)	552 ^a (1)	0.28	10.3	1.6	0.1	0.2	0.1
HC180-Wb-75	269 ^c (2)	319 ^b (3)	554 ^a (4)	0.32	10.2	2.3	0.3	0.1	0.1
HC-A-180–0.5	195 ^a (2)	293 ^a (4)	573 ^a (4)	0.22	7.5	6.9	5.0	2.1	0.6
HC-A-210–0.5	201 ^a (2)	281 ^a (2)	573 ^a (4)	0.16	9.8	4.2	2.8	0.9	0.9
HC-A-230–0.5	195 ^a (2)	429 ^c (1)	555 ^a (3)	0.17	9.9	5.4	3.8	1.1	0.8

^{a,b,c}Average values with standard deviations. Means with different superscript significantly differ ($p < 0.05$)

the conventional HTC an unsuitable strategy to reduce the ash agglomeration indexes.

4 Conclusions

The work evaluates two strategies to improve the characteristics of hydrochar from swine manure. Both treatments, acid-assisted HTC and post-treatment washing of hydrochar with HCl and acetone, improved hydrochar energy characteristics (HHV 19–25 MJ kg⁻¹) and ash content (7–17 wt.%). HCl-assisted treatment and HCl washing did not achieve a substantial reduction in the N and S contents of the hydrochar. Acetone washing achieved high efficiency in the removal of N- and S-containing organic compounds, decreasing the N and S contents in hydrochar to <2 and <0.15 wt.%, respectively, significantly improving the C content (~47 wt.%) and HHV (~19 MJ kg⁻¹). These materials also showed a low propensity to ash agglomeration and fouling. Acetone post-treatment of hydrochar proved to be a suitable strategy to improve the characteristics of hydrochar for industrial use as a biofuel.

Acknowledgements Authors greatly appreciate funding from Spain's MICINN (PID2019-108445RB-I00), MINECO (PDC2021-120755-I00 and TED2021-130287B-I00), Madrid Regional Government (Project S2018/EMT-4344), and Grupo Kerbest Company. R.P. Ipiales acknowledges the financial support from the Community of Madrid (IND2019/AMB-17092) and Arquimea Agrotech Company.

Author contribution Ricardo Paul Ipiales: investigation, formal analysis, writing—original draft. Andres Sarrion: investigation, formal analysis, writing—original draft. Elena Diaz: funding acquisition, writing—review and editing, supervision. Emiliano Diaz-Portuondo: writing—review and editing, supervision. Angel F. Mohedano: conceptualization, funding acquisition, methodology, resources, writing—review and editing, supervision, project administration. Angeles de la Rubia: conceptualization, formal analysis, funding acquisition, methodology, resources, writing—review and editing, supervision.

Funding Open Access funding provided thanks to the CRUE-CSIC agreement with Springer Nature.

Data availability Not applicable.

Declarations

Ethical approval Not applicable.

Competing interests The authors declare no competing interests.

Open Access This article is licensed under a Creative Commons Attribution 4.0 International License, which permits use, sharing, adaptation, distribution and reproduction in any medium or format, as long as you give appropriate credit to the original author(s) and the source, provide a link to the Creative Commons licence, and indicate if changes were made. The images or other third party material in this article are included in the article's Creative Commons licence, unless indicated otherwise in a credit line to the material. If material is not included in the article's Creative Commons licence and your intended use is not

permitted by statutory regulation or exceeds the permitted use, you will need to obtain permission directly from the copyright holder. To view a copy of this licence, visit <http://creativecommons.org/licenses/by/4.0/>.

References

1. European Statistics-Eurostat (2017) Agricultural census 2020. Edition, Statistical books eurostat
2. European Statistics-Eurostat (2020) Energy, transport and environment statistics. Edition, Statistical books eurostat
3. Ekpo U, Ross AB, Camargo-Valero MA, Fletcher LA (2016) Influence of pH on hydrothermal treatment of swine manure: impact on extraction of nitrogen and phosphorus in process water. *Bioresour Technol* 214:637–644. <https://doi.org/10.1016/j.biortech.2016.05.012>
4. Wei Y, Liang Z, Zhang Y (2022) Evolution of physicochemical properties and bacterial community in aerobic composting of swine manure based on a patent compost tray. *Bioresour Technol* 343:126136. <https://doi.org/10.1016/j.biortech.2021.126136>
5. European Statistics-Eurostat (2018) Agriculture-greenhouse gas emission statistics. Edition, Statistical books eurostat
6. Kelessidis A, Stasinakis AS (2012) Comparative study of the methods used for treatment and final disposal of sewage sludge in European countries. *Waste Manag* 32:1186–1195. <https://doi.org/10.1016/j.wasman.2012.01.012>
7. Zahedi S, Gros M, Petrović M, Balcazar, JL, Pijuan M (2022) Anaerobic treatment of swine manure under mesophilic and thermophilic temperatures: fate of veterinary drugs and resistance genes. *Sci Total Environ* 818. <https://doi.org/10.1016/j.scitotenv.2021.151697>
8. Imeni SM, Pelaz L, Corchado-lopo C et al (2019) Techno-economic assessment of anaerobic co-digestion of livestock manure and cheese whey (Cow, Goat & Sheep) at small to medium dairy farms. *Bioresour Technol* 291:121872. <https://doi.org/10.1016/j.biortech.2019.121872>
9. Goldfarb JL, Hubble AH, Ma Q et al (2022) Valorization of cow manure via hydrothermal carbonization for phosphorus recovery and adsorbents for water treatment. *J Environ Manage* 308:114561. <https://doi.org/10.1016/j.jenvman.2022.114561>
10. Ipiales RP, de la Rubia MA, Diaz E et al (2021) Integration of hydrothermal carbonization and anaerobic digestion for energy recovery of biomass waste: an overview. *Energy Fuels* 35:17032–17050. <https://doi.org/10.1021/acs.energyfuels.1c01681>
11. Lentz Z, Kolar P, Classen JJ (2019) Valorization of swine manure into hydrochars. *Processes* 1–12. <https://doi.org/10.3390/pr7090560>
12. Qaramaleki SV, Villamil JA, Mohedano AF, Coronella CJ (2020) Factors Affecting solubilization of phosphorus and nitrogen through hydrothermal carbonization of animal manure. *ACS Sustain Chem Eng* 8:12462–12470. <https://doi.org/10.1021/acsschemeng.0c03268>
13. Aragón-Briceño CI, Grasham O, Ross AB et al (2020) Hydrothermal carbonization of sewage digestate at wastewater treatment works: influence of solid loading on characteristics of hydrochar, process water and plant energetics. *Renew Energy* 157:959–973. <https://doi.org/10.1016/j.renene.2020.05.021>
14. Gaur RZ, Khoury O, Zohar M et al (2020) Hydrothermal carbonization of sewage sludge coupled with anaerobic digestion: integrated approach for sludge management and energy recycling. *Energy Convers Manag* 224:113353. <https://doi.org/10.1016/j.enconman.2020.113353>
15. Mannarino G, Sarrion A, Diaz E et al (2022) Improved energy recovery from food waste through hydrothermal carbonization and anaerobic digestion. *Waste Manag* 142:9–18. <https://doi.org/10.1016/J.WASMAN.2022.02.003>

16. Zhang Z, Yang J, Qian J et al (2021) Biowaste hydrothermal carbonization for hydrochar valorization: skeleton structure, conversion pathways and clean biofuel applications. *Bioresour Technol* 324:124686. <https://doi.org/10.1016/j.biortech.2021.124686>
17. Tayibi S, Monlau F, Marias F et al (2021) Coupling anaerobic digestion and pyrolysis processes for maximizing energy recovery and soil preservation according to the circular economy concept. *J Environ Manage* 279:111632. <https://doi.org/10.1016/j.jenvman.2020.111632>
18. Heidari M, Dutta A, Acharya B, Mahmud S (2019) A review of the current knowledge and challenges of hydrothermal carbonization for biomass conversion. *J Energy Inst* 92:1779–1799. <https://doi.org/10.1016/j.joei.2018.12.003>
19. Ipiates RP, Mohedano AF, Diaz E, de la Rubia MA (2022) Energy recovery from garden and park waste by hydrothermal carbonisation and anaerobic digestion. *Waste Manag* 140:100–109. <https://doi.org/10.1016/j.wasman.2022.01.003>
20. Gao L, Volpe M, Lucian M et al (2019) Does hydrothermal carbonization as a biomass pretreatment reduce fuel segregation of coal-biomass blends during oxidation? *Energy Convers Manag* 181:93–104. <https://doi.org/10.1016/j.enconman.2018.12.009>
21. Marin-Batista JD, Villamil JA, Rodriguez JJ et al (2019) Valorization of microalgal biomass by hydrothermal carbonization and anaerobic digestion. *Bioresour Technol* 274:395–402. <https://doi.org/10.1016/j.biortech.2018.11.103>
22. Reza MT, Freitas A, Yang X et al (2016) Hydrothermal carbonization (HTC) of cow manure: carbon and nitrogen distributions in HTC products. *Environ Prog Sustain Energy* 35:1002–1011. <https://doi.org/10.1002/ep.12312>
23. Sarrion A, de la Rubia A, Coronella C, Mohedano AF, Diaz E (2022) Acid-mediated hydrothermal treatment of sewage sludge for nutrient recovery. *Sci Total Environ* 156494. <https://doi.org/10.1016/j.scitotenv.2022.156494>
24. Dai L, Yang B, Li H et al (2017) A synergistic combination of nutrient reclamation from manure and resultant hydrochar upgradation by acid-supported hydrothermal carbonization. *Bioresour Technol* 243:860–866. <https://doi.org/10.1016/j.biortech.2017.07.016>
25. Xiong J, Chen S, Wang J, Wang Y, Fang X, Huang H (2021) Speciation of main nutrients (N/P/K) in hydrochars produced from the hydrothermal carbonization of swine manure under different reaction temperatures. *Materials (Basel)* 14. <https://doi.org/10.3390/ma14154114>
26. Pecchi M, Baratieri M, Goldfarb JL, Maag AR (2022) Effect of solvent and feedstock selection on primary and secondary chars produced via hydrothermal carbonization of food wastes. *Bioresour Technol* 348:126799. <https://doi.org/10.1016/j.biortech.2022.126799>
27. Puccini M, Ceccarini L, Antichi D, Seggiani M, Tavarini S, Latorre MH, Vitolo S (2018) Hydrothermal carbonization of municipal woody and herbaceous prunings: hydrochar valorisation as soil amendment and growth medium for horticulture. *Sustain* 10. <https://doi.org/10.3390/su10030846>
28. ASTM (2015) Standard test methods for proximate analysis of coal and coke by macro thermogravimetric analysis. *Method D7582–15*. ASTM-International 5:1–9. <https://doi.org/10.1520/D7582-15>
29. Zhang D, Han P, Yang R et al (2021) Fuel properties and combustion behaviors of fast torrefied pinewood in a heavily loaded fixed-bed reactor by superheated steam. *Bioresour Technol* 342:125929. <https://doi.org/10.1016/j.biortech.2021.125929>
30. Cao Z, Hülsemann B, Wüst D et al (2021) Effect of residence time during hydrothermal carbonization of biogas digestate on the combustion characteristics of hydrochar and the biogas production of process water. *Bioresour Technol* 333:125110. <https://doi.org/10.1016/j.biortech.2021.125110>
31. Reza MT, Wirth B, Lüder U, Werner M (2014) Behavior of selected hydrolyzed and dehydrated products during hydrothermal carbonization of biomass. *Bioresour Technol* 169:352–361. <https://doi.org/10.1016/j.biortech.2014.07.010>
32. Reza MT, Uddin MH, Lynam JG et al (2014) Hydrothermal carbonization of loblolly pine: reaction chemistry and water balance. *Biomass Convers Biorefinery* 4:311–321. <https://doi.org/10.1007/s13399-014-0115-9>
33. Lucian M, Volpe M, Gao L et al (2018) Impact of hydrothermal carbonization conditions on the formation of hydrochars and secondary chars from the organic fraction of municipal solid waste. *Fuel* 233:257–268. <https://doi.org/10.1016/j.fuel.2018.06.060>
34. Smith AM, Ekpo U, Ross AB (2020) The influence of pH on the combustion properties of bio-coal following hydrothermal treatment of swine manure. *Energies* 13:1–20. <https://doi.org/10.3390/en13020331>
35. Baccile N, Antonietti M, Titirici MM (2010) One-step hydrothermal synthesis of nitrogen-doped nanocarbons: albumine directing the carbonization of glucose. *Chemsuschem* 3:246–253. <https://doi.org/10.1002/cssc.200900124>
36. Aragón-Briceño CI, Pozarlik AK, Bramer EA et al (2021) Hydrothermal carbonization of wet biomass from nitrogen and phosphorus approach: a review. *Renew Energy* 171:401–415. <https://doi.org/10.1016/j.renene.2021.02.109>
37. Regmi P, Garcia Moscoso JL, Kumar S et al (2012) Removal of copper and cadmium from aqueous solution using switchgrass biochar produced via hydrothermal carbonization process. *J Environ Manage* 109:61–69. <https://doi.org/10.1016/j.jenvman.2012.04.047>
38. Yang G, Liu H, Li Y et al (2022) Kinetics of hydrothermal carbonization of kitchen waste based on multi-component reaction mechanism. *Fuel* 324:124693. <https://doi.org/10.1016/j.fuel.2022.124693>
39. Zhang Z, Zhao Y, Wang T (2020) Spirulina hydrothermal carbonization: effect on hydrochar properties and sulfur transformation. *Bioresour Technol* 306:123148. <https://doi.org/10.1016/j.biortech.2020.123148>
40. Wang T, Zhai Y, Zhu Y et al (2018) Influence of temperature on nitrogen fate during hydrothermal carbonization of food waste. *Bioresour Technol* 247:182–189. <https://doi.org/10.1016/j.biortech.2017.09.076>
41. Xiao H, Zhai Y, Xie J et al (2019) Speciation and transformation of nitrogen for spirulina hydrothermal carbonization. *Bioresour Technol* 286:121385. <https://doi.org/10.1016/j.biortech.2019.121385>
42. Souad H née M, Boufadès D, Boussak H, et al (2021) Efficient removal of sulfur and nitrogen compounds from actual fuels by oxidation-extraction process using acids combination. *Mater Today Proc*. <https://doi.org/10.1016/j.matpr.2021.10.309>
43. Prado GHC, Rao Y, De Klerk A (2017) Nitrogen removal from oil: a review. *Energy Fuels* 31:14–36. <https://doi.org/10.1021/acs.energyfuels.6b02779>
44. Heilmann SM, Molde JS, Timler JG et al (2014) Phosphorus reclamation through hydrothermal carbonization of animal manures. *Environ Sci Technol* 48:10323–10329. <https://doi.org/10.1021/es501872k>
45. Reza MT, Lynam JG, Uddin MH, Coronella CJ (2013) Hydrothermal carbonization : fate of inorganics. *Biomass Bioenerg* 49:86–94. <https://doi.org/10.1016/j.biombioe.2012.12.004>
46. Wang R, Zhang L, Zhang C et al (2022) Selective extraction of precious metals in the polar aprotic solvent system: experiment and simulation. *Waste Manag* 153:1–12. <https://doi.org/10.1016/j.wasman.2022.08.012>
47. Lin W, Zhang RW, Jang SS et al (2010) Organic aqua regia-Powerful liquids for dissolving noble metals. *Angew Chemie Int Ed* 49:7929–7932. <https://doi.org/10.1002/anie.201001244>
48. Roncal-Herrero T, Rodríguez-Blanco JD, Benning LG, Oelkers EH (2009) Precipitation of iron and aluminum phosphates directly from aqueous solution as a function of temperature from 50 to 200 °C. *Cryst Growth Des* 9:5197–5205. <https://doi.org/10.1021/cg900654m>
49. Ahn H, Kim D, Lee Y (2020) Combustion characteristics of sewage sludge solid fuels produced by drying and hydrothermal

- carbonization in a fluidized bed. *Renew Energy* 147:957–968. <https://doi.org/10.1016/j.renene.2019.09.057>
50. Lang Q, Liu Z, Li Y et al (2022) Combustion characteristics, kinetic and thermodynamic analyses of hydrochars derived from hydrothermal carbonization of cattle manure. *J Environ Chem Eng* 10:106938. <https://doi.org/10.1016/j.jece.2021.106938>
51. Otero M, Sánchez ME, Gómez X (2011) Co-firing of coal and manure biomass: a TG-MS approach. *Bioresour Technol* 102:8304–8309. <https://doi.org/10.1016/j.biortech.2011.06.040>
52. Mäkelä M, Fullana A, Yoshikawa K (2016) Ash behavior during hydrothermal treatment for solid fuel applications. Part 1: Overview of different feedstock. *Energy Convers Manag* 121:402–408. <https://doi.org/10.1016/j.enconman.2016.05.016>
53. Mäkelä M, Yoshikawa K (2016) Ash behavior during hydrothermal treatment for solid fuel applications. Part 2: Effects of treatment conditions on industrial waste biomass. *Energy Convers Manag* 121:409–414. <https://doi.org/10.1016/j.enconman.2016.05.015>

Publisher's note Springer Nature remains neutral with regard to jurisdictional claims in published maps and institutional affiliations.